

Dark matter distribution in the Draco dwarf from velocity moments

Ewa L. Lokas,^{1,2} Gary A. Mamon^{2,3} and Francisco Prada⁴

¹Nicolaus Copernicus Astronomical Center, Bartycka 18, 00-716 Warsaw, Poland

²Institut d'Astrophysique de Paris (UMR 7095: CNRS & Université Pierre & Marie Curie), 98 bis Bd Arago, F-75014 Paris, France

³GEPH (UMR 8111: CNRS & Université Denis Diderot), Observatoire de Paris, F-92195 Meudon, France

⁴Instituto de Astrofísica de Andalucía (CSIC), Apartado Correos 3005, E-18080 Granada, Spain

11 April 2024

ABSTRACT

We study the distribution of dark matter in the Draco dwarf spheroidal galaxy by modelling the moments of the line-of-sight velocity distribution of stars obtained from new velocity data of Wilkinson et al. The luminosity distribution is approximated by a Sersic profile fitted to the data by Odenkirchen et al. We assume that the dark matter density profile is given by a formula with an inner cusp and an outer exponential cut-off, as recently proposed by Kazantzidis et al. as a result of simulations of tidal stripping of dwarfs by the potential of the Milky Way. The dark matter distribution is characterized by the total dark mass and the cut-off radius. The models have arbitrary velocity anisotropy parameter assumed to be constant with radius. We estimate the three parameters by fitting both the line-of-sight velocity dispersion and kurtosis profiles, which allows us to break the degeneracy between the mass distribution and velocity anisotropy. The results of the fitting procedure turn out to be very different depending on the stellar sample considered, that is on our choice of stars with discrepant velocities to be discarded as interlopers. For our most reliable sample, the model parameters remain weakly constrained, but the robust result is the preference for weakly tangential stellar orbits and high mass-to-light ratios. The best-fitting total mass is then $7 \times 10^7 M_\odot$, much lower than recent estimates, while the mass-to-light ratio is $M/L_V = 300$ and almost constant with radius. If the binary fraction in the stellar population of Draco turns out to be significant, the kurtosis of the global velocity distribution will be smaller and the orbits inferred will be more tangential, while the resulting mass estimate lower.

Key words: galaxies: Local Group { galaxies: dwarf { galaxies: clusters: individual: Draco { galaxies: fundamental parameters { galaxies: kinematics and dynamics { cosmology: dark matter

1 INTRODUCTION

Dwarf spheroidal galaxies are currently believed to be among the most dark matter dominated objects in the Universe (with mass-to-light ratios up to few hundred solar units) and therefore are of immediate interest when trying to test present theoretical predictions concerning the dark matter profiles. As dwarfs, they are also important for theories of structure formation, which suffer from the overabundance of subhaloes (Klypin et al. 1999).

The Draco dwarf spheroidal galaxy (hereafter, Draco)

is a generic example of this class of objects in the neighbourhood of the Galaxy and has been already the subject of extensive study. Recently, new radial-velocity observations of Draco have yielded a larger kinematic sample (Kleyna et al. 2002; Wilkinson et al. 2004) and the Sloan Digital Sky Survey has yielded a better determination of the luminosity profile and shape (Odenkirchen et al. 2001). Draco has also been examined for the presence of tidal tails which could indicate a kinematically perturbed state. For a long time it has been debated (e.g. Kleisen & Kroupa 1998; Kleisen & Zhao 2002) whether the large velocity dispersion measured in Draco is a result of significant dark matter content or a signature of tidal disruption by the Milky Way. New analyses by Piatek et al. (2002) and Kleisen, Gebel & Harbeck (2003) show that there is no evidence that tidal forces from

² E-mail: lokas@camk.edu.pl

y E-mail: gam@iap.fr

z E-mail: fprada@iaa.es

the Milky Way have disturbed the inner structure of Draco. In particular, Klessen et al. (2003) argue that models without any dark matter are unable to reproduce the narrow observed horizontal branch width of Draco. As we will show below, the truth may lie between these two pictures: Draco most probably is strongly dark matter dominated but still its outer edges could be affected by tidal interaction with the Milky Way producing a population of stars unbound to the dwarf.

One of the major methods to determine the dark matter content of galaxies and clusters is to study the kinematics of their observable discrete component: stars or galaxies, respectively. The method is based on the assumption that the positions and velocities of the component members trace the Newtonian gravitational potential of the object. If the object is in virial equilibrium the relation between those is described by the Jeans formalism. In the classical approach, such an analysis is restricted to solving the lowest order Jeans equation and modelling only the velocity dispersion profile. In previous papers (Lokas 2002; Lokas & Mamon 2003), building on the earlier work by Merrifield & Kent (1990) and van der Marel et al. (2000), we have extended the formalism to include the solutions of the higher-order Jeans equations describing the fourth velocity moment, the kurtosis.

The formalism has been successfully applied to study the dark matter distribution in the Coma cluster of galaxies (Lokas & Mamon 2003). We have shown that, for a restricted class of dark matter distributions motivated by the results of cosmological N -body simulations, the joint analysis of velocity dispersion and kurtosis allows us to break the usual degeneracy between the mass distribution and velocity anisotropy and constrain the parameters of the dark matter profile. Recently we have tested the reliability of this approach against a series of N -body simulations (Sanchis, Lokas & Mamon 2004) and verified that the method allows for typically accurate determinations of the mass, concentration and velocity anisotropy (albeit with a large scatter in concentration). In the present paper, encouraged by these successes, we apply the method to constrain the dark matter distribution in the Draco dwarf spheroidal galaxy.

The paper is organized as follows. In Section 2 we summarize the Jeans formalism for the calculation of the moments of the line-of-sight velocity distribution. In Section 3 we estimate the moments from the velocity data and discuss the associated difficulties caused by the possible presence of interlopers and binary stars. Section 4 describes our models for the luminosity and dark matter distributions. Results of fitting the models to the data are presented and discussed in Section 5. In Section 6 we comment on the possible origin of unbound stars in Draco and the concluding remarks follow in Section 7.

2 VELOCITY MOMENTS FROM THE JEANS FORMALISM

The Jeans formalism (e.g. Binney & Tremaine 1987) relates the velocity moments of a gravitationally bound object to the underlying mass distribution. We summarize here the formalism, as developed in Lokas (2002) and Lokas & Mamon (2003). The second σ_r^2 and fourth-order $\overline{v_r^4}$ radial ve-

locity moments obey the Jeans equations

$$\frac{d}{dr} \left(\sigma_r^2 \right) + \frac{2}{r} \sigma_r^2 + \frac{d}{dr} \left(\frac{\sigma_r^2}{r} \right) = 0 \quad (1)$$

$$\frac{d}{dr} \left(\overline{v_r^4} \right) + \frac{2}{r} \overline{v_r^4} + 3 \sigma_r^2 \frac{d}{dr} \left(\frac{\sigma_r^2}{r} \right) = 0 \quad (2)$$

where ρ is the 3D density distribution of the tracer population and Φ is the gravitational potential. The second equation was derived assuming the distribution function of the form $f(E; L) = f_0(E)L^{-2}$ and the anisotropy parameter relating the angular and radial r velocity dispersions

$$\beta = 1 - \frac{\sigma_\theta^2(r)}{\sigma_r^2(r)} \quad (3)$$

to be constant with radius. We will consider here $-1 < \beta < 1$ which covers all interesting possibilities from radial orbits ($\beta = 1$) to isotropy ($\beta = 0$) and circular orbits ($\beta = -1$).

The solutions to equations (1)–(2) are

$$\sigma_r^2(\beta = \text{const}) = r^2 \int_0^1 \frac{dr}{r^2} \quad (4)$$

$$\overline{v_r^4}(\beta = \text{const}) = 3r^2 \int_0^1 \frac{\overline{v_r^4}(r)}{r^2} dr : \quad (5)$$

Projecting along the line of sight we obtain the observable quantities

$$\sigma_{\text{los}}^2(R) = \frac{2}{I(R)} \int_0^R \frac{\sigma_r^2}{r^2} \left(1 - \frac{R^2}{r^2} \right) dr \quad (6)$$

$$\overline{v_{\text{los}}^4}(R) = \frac{2}{I(R)} \int_0^R \frac{\overline{v_r^4}}{r^2} \frac{R^2}{R^2} g(r; R; \beta) dr \quad (7)$$

where

$$g(r; R; \beta) = 1 - 2 \frac{R^2}{r^2} + \frac{(1 + \beta) R^4}{2 r^4} ; \quad (8)$$

$I(R)$ is the surface distribution of the tracer and R is the projected radius.

Introducing equations (4)–(5) into (6)–(7) and inverting the order of integration, the calculations of σ_{los} and $\overline{v_{\text{los}}^4}$ can be reduced to one- and two-dimensional numerical integrals respectively (see the appendix of Mamon & Lokas 2005 for a simpler expression for σ_{los}). In the following we will refer to the fourth moment in the form of kurtosis

$$\kappa_{\text{los}}(R) = \frac{\overline{v_{\text{los}}^4}(R)}{\sigma_{\text{los}}^4(R)} ; \quad (9)$$

whose value is 3 for a Gaussian distribution.

3 VELOCITY MOMENTS FROM OBSERVATIONS

Fig. 1 shows the heliocentric velocities and projected distances from the centre of 207 stars with good velocity measurements from Wilkinson et al. (2004). The distances are calculated assuming that the centre of Draco is at $RA = 17^h 20^m 13.2^s$, $Dec = 57^\circ 54' 54.0''$ (J2000) (Odenkirchen et al. 2001). The sample was obtained from the original sample of 416 velocities stars observed in the direction of Draco by cutting out all objects with velocities differing by more than 39 km s^{-1} from Draco's mean velocity of 291 km s^{-1} . This choice was motivated by the assumption that the velocity distribution is Gaussian with a maximum dispersion of 13

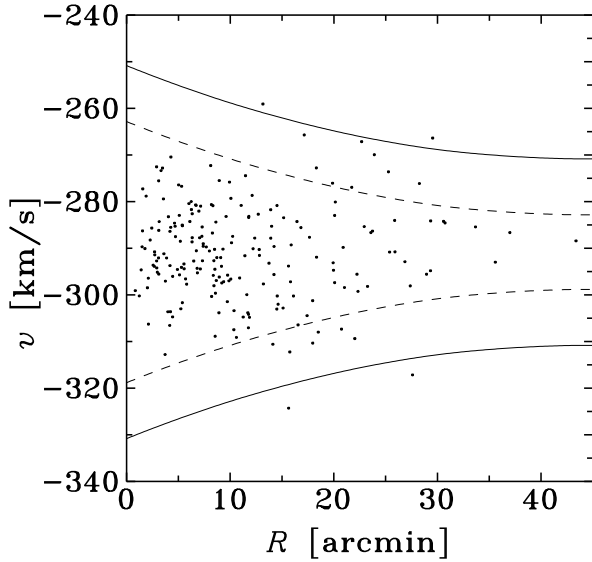


Figure 1. Heliocentric velocities versus distances from the centre of Draco for 207 stars. The solid (dashed) curves separate 203 (189) stars counted as members of the galaxy from the 4 (18) supposed interlopers.

km s^{-1} . We should however still take into account the possibility that some of the 207 stars are interlopers unbound to the gravitational potential of the galaxy. Prida et al. (2003) discussed the issue thoroughly in the case of isolated galaxies in the Sloan Digital Sky Survey (SDSS) and showed that the presence of interlopers can affect significantly the velocity dispersion and therefore the inferred mass distribution in the galaxy. This effect is especially important in the case of small samples like the present one.

The problem has been also discussed by Mayer et al. (2001) who showed (see Fig. 26 of the published version of their paper) how the velocity dispersion profiles of the dwarf spheroidal galaxies can be affected if the line of sight is along one of the tidal tails: while the intrinsic dispersion profile is declining, the observed one, due to the presence of unbound stars in the tail, is much higher and increasing. They state explicitly that a velocity dispersion that increases outside the core of the dwarf should be considered as a result of possible contamination by tidal tails. We address the issue in more detail in Section 6.

Judging by the shape of the diagram shown in Fig. 1 and comparing it with the expected appearance of gravitationally bound object in velocity space we immediately see that there are at least four stars with discrepant velocities: they have been separated from the main body of the galaxy by the solid lines. An even more stringent, but still arbitrary choice, with 14 more stars excluded, is shown with dashed lines. The lines were drawn symmetrically with respect to the mean systemic velocity of 291 km s^{-1} , as estimated from the total sample with 207 stars. Since we have no possibility of determining a priori which stars are actually bound to the galaxy we calculate the velocity moments using the three samples with 207, 203 and 189 velocities obtained in this way.

In the estimation of the moments, we follow the Appendix in Lokas & Mamon (2003) neglecting the small errors

in the velocity measurements. We divide the sample into 5 radial bins each containing 37–43 stars (depending on the sample: 207 stars are divided into bins with 41 + 43 velocities, 203 stars into 41 + 39 velocities and 189 stars into 38 + 37 velocities). The most natural estimators of the variance and kurtosis from a sample of n line-of-sight velocity measurements v_i are

$$S^2 = \frac{1}{n} \sum_{i=1}^n (v_i - \bar{v})^2 \quad (10)$$

and

$$K = \frac{\frac{1}{n} \sum_{i=1}^n (v_i - \bar{v})^4}{(S^2)^2} \quad (11)$$

where

$$\bar{v} = \frac{1}{n} \sum_{i=1}^n v_i \quad (12)$$

is the mean of stellar velocities in the sample. The distributions of these estimators for our binning of stars, i.e. when $n = 40$, can be investigated by running Monte Carlo simulations selecting $N = 10^4$ times $n = 40$ numbers from a Gaussian distribution with zero mean and dispersion of unity (see Lokas & Mamon 2003). One can then construct unbiased and nearly Gaussian-distributed estimators of line-of-sight velocity dispersions and kurtosis-like variable k

$$s = \frac{n}{n-1} S^2 \quad (13)$$

$$k = \log \frac{3}{2.75} K \quad (14)$$

The factor $n-1$ in equation (13) is the well known correction for bias when estimating the sample variance, valid independently of the underlying distribution. In (14) the factor $3/2.75$ corrects for the bias in the kurtosis estimate, i.e. unbiased estimate of kurtosis is $K^0 = 3K/2.75$, while the rather complicated function of K^0 assures that the sampling distribution of k is approximately Gaussian. We find that the standard errors in the case of s are of the order of 11 percent while in the case of k are approximately 2 percent. In the following we assign these errors to our data points.

We checked that even for weakly non-Gaussian velocity distributions, such as following from the present data, estimators s and k are Gaussian-distributed to a very good approximation and very weakly correlated with the correlation coefficient $\rho_{sk} = 0.07$. We can therefore assume that, to a good approximation, all of our data points measuring velocity dispersion and kurtosis will be independent, which justifies the use of standard χ^2 minimization to fit the models to the data.

Apart from the sampling distributions discussed above, our estimates of the velocity moments can be affected by the presence of binary stars. Contrary to the studies of galaxy clusters, where galaxy pairs are rare and can be rather easily identified and eliminated from the sample, in the case of stellar systems, such as Draco, binaries can be identified only through long-term monitoring of the whole stellar sample. In the sample of Wilkinson et al. (2004) such repeated measurements exist only for 66 stars and among those only a few are probable binaries, i.e. the differences between their velocity measurements are too big to be accounted for by the

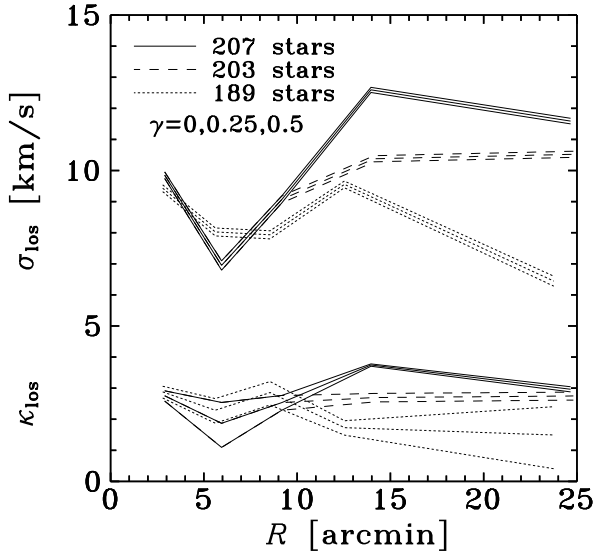


Figure 2. Velocity moments calculated from the three samples of 207 (solid lines), 203 (dashed lines) and 189 stars (dotted lines) and different binary fraction $\gamma = 0, 0.25$ and 0.5 . In each triplet the highest line corresponds to $\gamma = 0$ (no correction for binaries).

measurement errors. Given the uncertainties in our knowledge of the binary population in Draco, we assume that the binary fraction is negligible ($\gamma = 0$), but we discuss briefly below how a significant amount of binaries could affect the results.

De Rijcke & Dejonghe (2002) studied the influence of the binary population on the observed line-of-sight velocity moments and found (see their Fig. 15) that for stellar systems with $\sigma_{\text{los}} \approx 9 \text{ km s}^{-1}$, such as Draco, the observed (Gaussian) dispersion is mildly affected by the presence of binaries in comparison with the intrinsic stellar velocity dispersion. However, the kurtosis value turns out to be more affected. Inverting the formulae (55) in De Rijcke & Dejonghe (2002) we find that given the line-of-sight velocity moments of the binary population, σ_b and κ_b we can calculate the intrinsic moments of the stars σ_i and κ_i from the observed ones σ_o and κ_o .

$$\sigma_i^2 = \sigma_o^2 - \sigma_b^2 \quad (15)$$

$$\kappa_i = \kappa_o - \frac{\sigma_o^4}{\sigma_i^4} - \frac{\sigma_b^4}{\sigma_i^4} - 6 \frac{\sigma_o^2 \sigma_b^2}{\sigma_i^6} \quad (16)$$

We adopt the values of $\sigma_b = 2.87 \text{ km s}^{-1}$ and $\kappa_b = 86.89$, as obtained by De Rijcke & Dejonghe (2002) for their standard binary population model. Having calculated the observed moments $\sigma_o = \sigma$ and $\kappa_o = K = 3K = 2.75$ from equations (10)–(13) we obtain the intrinsic values from equations (15)–(16).

The uncertainties in the determination of the velocity moments are illustrated in Fig. 2. The solid lines join the moments calculated in five bins with all 207 velocities, the dashed and dotted ones with 203 and 189 velocities respectively. The three curves of each kind correspond to the binary fraction $\gamma = 0, 0.25$ and 0.5 , from the highest to the lowest, i.e. correcting for binaries decreases the values of moments. The estimates overlap for the first three bins of samples with 207 and 203 stars because none of the supposed

interlopers fall there, the small differences in the case of the sample with 189 stars are due to different number of stars per bin. For the two outer bins the situation is however very different, with all 207 stars the velocity dispersion is much larger than for 203 and 189 stars. We note that although the profile for 207 stars decreases in the last bin, there is no sudden drop in velocity dispersion as found by Wilkinson et al. (2004). This is mainly due to our larger number of stars per bin.

As demonstrated by Fig. 2, except for the most numerous sample with 207 stars, the kurtosis values typically fall below the Gaussian value of 3. Such kurtosis signifies a centrally flattened velocity distribution in comparison with the Gaussian. It is worth noting that the behaviour of the kurtosis profile for the sample with 189 stars (close to Gaussian value in the centre and lower values at larger distances) is similar to the one found in the case of distribution of galaxy velocities in the Coma cluster (Lokas & Mamon 2003). Decreasing kurtosis values seem also to be typical properties of the projected velocity distributions of particles in simulated dark matter haloes as demonstrated by the studies of Sánchez et al. (2004), Kazantzidis, Mamonian & Moore (2004) and Diemand, Moore & Stadel (2004).

Our purpose now is to reproduce the observed profiles of velocity moments using models described in the next Section.

4 DISTRIBUTIONS OF STARS AND DARK MATTER

4.1 Stars

The distribution of stars is modelled in the same way as in Lokas (2001, 2002) i.e. by the Sersic profile (Sersic 1968)

$$I(R) = I_0 \exp \left[- \left(\frac{R}{R_s} \right)^{1+m} \right]; \quad (17)$$

where I_0 is the central surface brightness and R_s is the characteristic projected radius of the Sersic profile. The 3D luminosity density $\rho(r)$ is obtained from $I(R)$ by deprojection

$$\rho(r) = \frac{1}{r} \int_r^\infty \frac{dI}{dR} R \frac{dR}{R^2 r^2}; \quad (18)$$

For a wide range of values $1 \leq m \leq 10$ found to fit the light distribution in elliptical and spheroidal galaxies an excellent approximation for $\rho(r)$ is provided by (Lima Neto, Gerbal & Marquez 1999)

$$\rho(r) = \rho_0 \frac{r}{R_s}^p \exp \left[- \frac{r}{R_s}^{1+m} \right] \quad (19)$$

$$\rho_0 = \frac{I_0 (2m)}{2R_s [(3-p)m]} \\ p = 1.0 - 0.6097m + 0.05463m^2;$$

The mass distribution of stars following from (19) is

$$M(r) = M_s \frac{[(3-p)m; (r/R_s)^{1+m}]}{[(3-p)m]}; \quad (20)$$

where $M_s = L_{\text{tot}}$ is the total mass of stars, with $\gamma = \text{const}$ the mass-to-light ratio for stars, L_{tot} the total luminosity of the galaxy, and $\Gamma(x) = \int_0^\infty e^{-t} t^{x-1} dt$ is the incomplete gamma function.

Table 1. Adopted parameters of the Draco dwarf.

parameter	value
luminosity $L_{\text{tot},V}$	$2.2 \times 10^5 L_\odot$
distance d	80 kpc
distance modulus $m - M$	19.5
stellar mass-to-light ratio ν	$3 M_\odot = L_\odot$
stellar mass M_s	$6.6 \times 10^5 M_\odot$
Sersic radius R_s	7.3 arcmin
Sersic parameter m	0.83

Odenkirchen et al. (2001) find that their data for the surface density of stars in Draco are best fitted (for sample S1) with $m = 1.2$ ($m = 0.83$) and the Sersic radius $R_s = 7.3$ arcmin. We will adopt these values here assuming that the population of stars is uniform and therefore the distribution of stars can be translated to the surface luminosity in any band just by adjusting the normalization I_0 . We note that the surface density distribution estimated by Odenkirchen et al. (2001) agrees well with the independent estimates by Piatek et al. (2002) from a different data set. In particular, both groups find the distribution to fall sharply at large distances thus contradicting the earlier estimates of Irwin & Hatzidimitriou (1995) who found a flattening profile which could point towards the presence of tidal tails.

We adopt the apparent magnitude of Draco in the i -band $m_i = 10.49$ following Odenkirchen et al. (2001). Using their formula (8) relating i and I magnitudes, and assuming $V - I = 1$ from the colour-magnitude diagram in Fig. 5 of Bonanos et al. (2004) we find $i - I = 0.52$ in agreement with Table 3 of Fukugita, Shimazaki & Ichikawa (1995) and $V - i = 0.48$. Taking a distance estimate for Draco of $d = 80$ kpc (Aparicio, Carrera & Martinez-Delgado 2001), corresponding to the distance modulus $m - M = 19.5$, we obtain the total luminosity of Draco in the V -band of $L_{\text{tot},V} = 2.2 \times 10^5 L_\odot$, which is somewhat larger than the earlier estimate of $L_{\text{tot},V} = 1.8 \times 10^5 L_\odot$ by Irwin & Hatzidimitriou (1995). We note that the adopted distance agrees well with the most recent estimate by Bonanos et al. (2004) who found $m - M = 19.4$ once an appropriate (for their method of distance scale calibration) correction of 0.1 mag is applied.

In order to estimate the mass in stars, we need to adopt the stellar mass-to-light ratio in V -band, which for dwarf spheroidals is believed to be similar to that of globular clusters $\nu = (1 - 3) M_\odot = L_\odot$. Although the age and metallicity of Draco stellar population are reasonably well known, the predicted values of ν are still uncertain and different stellar population synthesis codes and different initial mass functions tend to produce results discrepant at least by a factor of 2 (Schulz et al. 2002). Since we do not want to overestimate the amount of dark matter in our modelling, and keeping in mind that there is probably a significant contribution from ionized gas in Draco (up to $2 \times 10^5 M_\odot$, Gallagher et al. 2003) we take a higher value $\nu = 3 M_\odot = L_\odot$ so that our total stellar mass will be $M_s = \nu L_{\text{tot},V} = 6.6 \times 10^5 M_\odot$. All the parameters of Draco discussed in this Section are summarized in Table 1.

We also note that the ellipticity of the surface density distribution of stars in Draco is low, $e = 0.3$ (Odenkirchen et al. 2001; Piatek et al. 2002), so the galaxy is likely to be close to spherical, which makes the use of our spherical

models justified and reduces the chance that non-sphericity will affect our results (see Sanchis et al. 2004).

4.2 Dark matter

Recently, Kazantzidis et al. (2004) performed a series of N -body simulations of the evolution of a subhalo in the field of a larger halo of a galaxy. Their Draco-like object initially had an NFW density distribution (Navarro, Frenk & White 1997) but due to tidal interactions with a galaxy similar to the Milky Way lost some of its mass. The resulting, tidally stripped, density profile retained the initial r^{-1} cusp at the centre but developed an exponential cut-off at large distances and could be well approximated by a formula

$$\rho_d(r) = C r^{-1} \exp\left(-\frac{r}{r_b}\right); \quad (21)$$

where r_b is the break radius at which the cut-off occurs. The dark mass distribution associated with the density profile (21) is

$$M_d(r) = M_D \left[1 - \exp\left(-\frac{r}{r_b}\right) \right] + \frac{r}{r_b}; \quad (22)$$

which we have normalized with M_D , the total dark mass of the halo. (Note that contrary to the standard NFW distribution, for this profile the mass converges.) With this normalization, the constant in equation (21) becomes $C = M_D = (4 r_b^2)$.

It is still debated whether tidal interaction of dwarfs with gravitational potential of their host galaxies is likely to flatten the inner profile of their halo. Although Kazantzidis et al. (2004) find that the cusp is preserved over a few orbital periods, there are also claims that it can be flattened (Hayashiet al. 2003). One may also question the assumption of a cuspy initial profile in the light of recent re-nements in studies of density profiles of dark matter haloes which find a flattening profile in the centre (Navarro et al. 2004; Stoehr 2005). We believe however that, from the point of view of the present study, the inner slope of the halo is not really important since it should not affect our conclusions concerning the total mass or anisotropy. In the study of the dark matter distribution in the Coma cluster Lokas & Mamon (2003) considered a generalized profile with an arbitrary inner slope and found almost the same best-fitting mass and anisotropy for flat and cuspy inner profiles.

5 RESULTS AND DISCUSSION

In this Section, we report our attempts to reproduce the observed velocity moments shown in Fig. 2 using models described by equations (6)–(9), with the mass distribution given by the sum of the two contributions (20) and (22) discussed in the previous Section:

$$M(r) = M_*(r) + M_d(r); \quad (23)$$

The density profile $\rho(r)$ of the tracer population of stars is given by equation (19) and the surface brightness $I(R)$ by the Sersic formula (17) with $m = 0.83$. As discussed by Lokas & Mamon (2003) and Sanchis et al. (2004), while studying velocity dispersion is useful to constrain the mass, the kurtosis is mostly sensitive to the velocity anisotropy. However, as will become clear below, when the anisotropy is

constrained, the degeneracy between the mass distribution and velocity anisotropy, usually present when only velocity dispersion is considered, is broken and the parameters describing the mass distribution can also be constrained.

We begin by fitting the line-of-sight velocity dispersion profiles shown by the upper curves in Fig. 2 and adjusting three parameters: the anisotropy parameter β , total dark mass in units of the total stellar mass $M_D = M_S$ and the break radius of the dark matter profile in units of the Sersic radius $r_b = R_S$ measuring the extent of the dark matter halo. The results for our different samples of 189, 203 and 207 stars are shown in Fig. 3 so that the best-fitting $M_D = M_S$ (upper panel) and the velocity anisotropy parameter β (middle panel) are displayed as a function of $r_b = R_S$. The thinner lines in the lower panel of Fig. 3 show the corresponding goodness of fit χ^2 . The lower panel of Fig. 3 proves that none of the parameters can be constrained from the analysis of velocity dispersion alone: χ^2 is flat for a large range of $r_b = R_S$ and does not discriminate between different values of the parameters.

As discussed in Section 3, the sampling distributions of \log_{10} and $(\log_{10})^{1-10}$ are independent to a good approximation, hence we can use the same minimization scheme to find joint constraints following from fitting both quantities. Before that, however, we calculate χ^2 using the total of 10 data points for each sample of 189, 203 and 207 stars for the values of the parameters dictated by the best fit to the velocity dispersion data in Fig. 3. The results are shown in the lower panel of the Figure with thicker lines. We immediately see that χ^2 has a minimum only for our sample with 189 stars. For the other samples its values decrease for increasing $r_b = R_S$ and $M_D = M_S$ and their minimum is not reached even if we go to incredibly high masses like $M_D = M_S = 10^6$. Such masses would be comparable to the mass of the Milky Way itself.

The reason for this behaviour can be understood by referring to Fig. 4, where we plot the predicted velocity moments for different values of the anisotropy parameter β . For simplicity we assumed the mass distribution as obtained from the fit to the sample of 189 stars (see eq. [24] below). It should be kept in mind that the kurtosis profile depends mainly on anisotropy, while the velocity dispersion is degenerate in anisotropy versus mass (taking a more extended mass distribution for the plot would result in a more strongly increasing \log_{10} in analogy to more tangential orbits but the kurtosis profile would remain unaltered). As seen in the Figure and already discussed by Lokas & Mamon (2003) and Sanchis et al. (2004) (see also Gerhard 1993), tangential orbits produce a decreasing kurtosis profile, as is indeed observed for the sample with 189 stars. But the kurtosis values of samples with 207 and 203 stars are rather high (close to Gaussian) and therefore values close to isotropic or mildly radial are preferred while increasing velocity dispersion profiles require tangential orbits (see the middle panel of Fig. 3). Without tangential orbits such velocity dispersion profiles could only be reproduced if the mass profiles are extended and this is the reason the χ^2 values decrease for higher masses and break radii. This indicates that the samples with 207 and 203 stars should be treated with caution. In the case of the sample with 203 stars a reasonably good fit to both moments can be obtained, although for rather high masses. For the sample with 207 stars however,

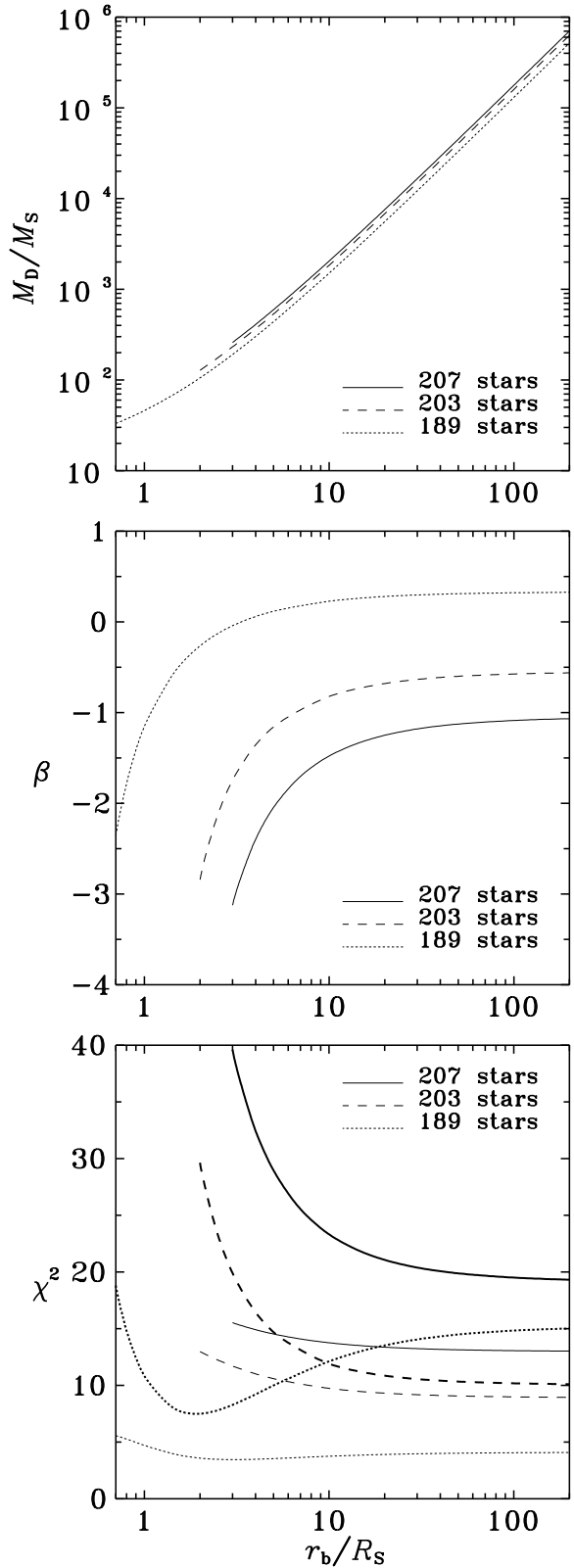


Figure 3. Results of fitting only the line-of-sight velocity dispersion data. The best fitting parameters $M_D = M_S$ and β are shown in the two upper panels as a function of $r_b = R_S$ for different stellar samples. The thinner lines in the lower panel give the goodness of fit χ^2 from fitting velocity dispersion. The thicker lines show χ^2 values obtained for the same parameters if the kurtosis data are included.

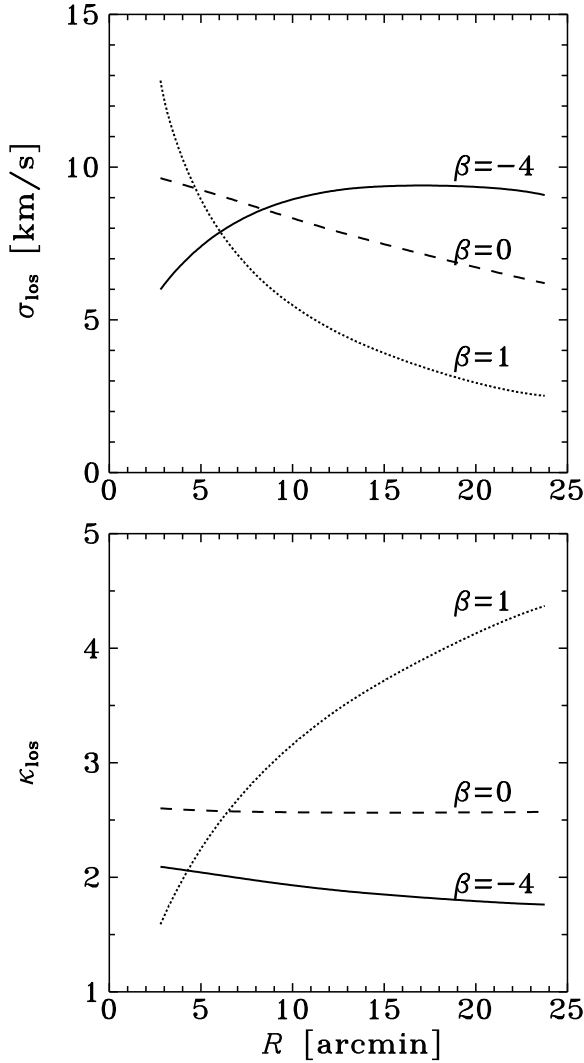


Figure 4. Line-of-sight velocity dispersion σ_{los} (upper panel) and kurtosis (lower panel) as a function of projected radius, for different anisotropies: radial ($\beta = 1$), isotropic ($\beta = 0$) and moderately tangential ($\beta = -4$, i.e. $\sigma_r = 2.2\sigma_t$). The mass distribution is given by the best-fit for the sample with 189 stars, eq. (24).

the fit is bad and improves only for incredibly high masses, which may indicate that this sample yields inconsistent velocity dispersion and kurtosis profiles and therefore that it almost certainly includes unbound stars.

One may ask to what extent this conclusion depends on our assumed constant anisotropy. It has recently been verified using the cosmological N-body simulations (Wojtak et al. 2005) that the radial velocity moments of bound objects, eqs. (4) and (5), are actually sensitive to the local value of the anisotropy parameter. We expect this to be true also for the projected moments since the dominant contribution to the projected moment near the centre of the object comes from the stars that are actually near the centre because they are more numerous than the foreground and background stars, while the value of the projected moment at some projected distance R from the centre is affected only by stars located at true distances $r \geq R$. This behaviour in the case of velocity dispersion has been explicitly verified by Lokas &

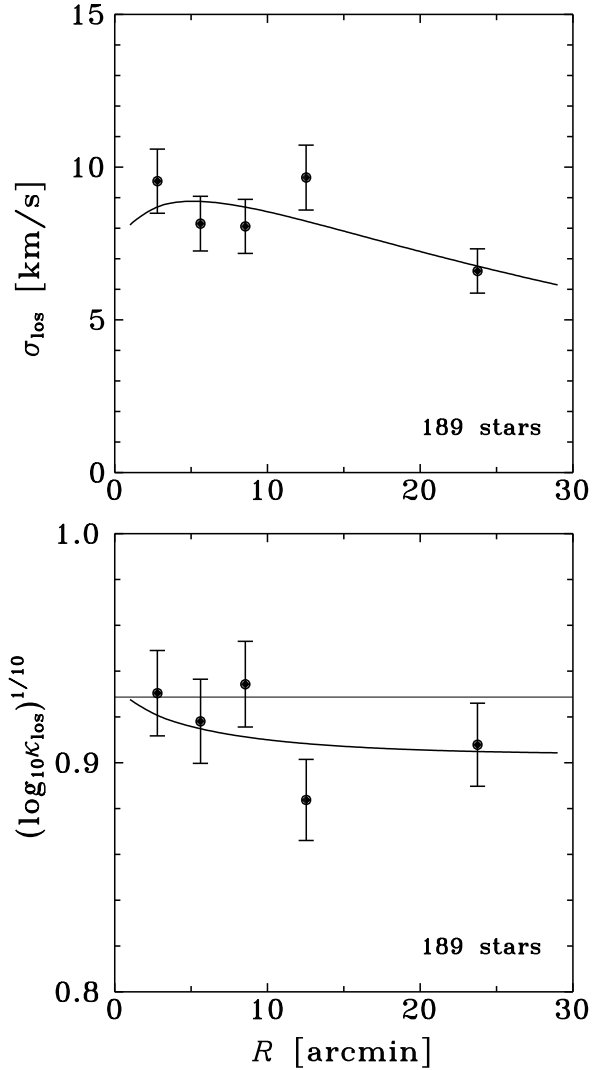


Figure 5. Line-of-sight velocity dispersion σ_{los} (upper panel) and dimensionless line-of-sight kurtosis parameter $(\log_{10} \kappa_{\text{los}})^{1/10}$ (lower panel) with 1 σ error bars for the sample with 189 stars. The curves represent the best-fitting model. The thin horizontal line in the lower panel marks the value of $(\log 3)^{1/10} = 0.93$ corresponding to the Gaussian velocity distribution.

Mamon (2001) for the Ostriker-Merritt anisotropy (see their Figures 1 and 6). We therefore expect that the anisotropy parameter changing e.g. from isotropic orbits near the centre to tangential orbits at larger distances would produce σ_{los} and κ_{los} profiles following the dashed line at small R and solid line at large R in the upper and lower panel of Fig. 4 respectively. The kurtosis profile would then decrease even more strongly and the conclusion concerning the samples with 203 and 207 stars would be similar as in the case of constant β . Interestingly, the dispersion profile interpolating between the dashed and solid line in the upper panel of Fig. 4 could reproduce the dip in the velocity dispersion profile seen in the data for all samples (see Fig. 2) and preserved for different binnings of the stars.

We therefore conclude that the choice of the sample of stars is the dominant source of uncertainty when trying to determine the mass distribution in Draco. In the following

we will only consider the sample with 189 stars and investigate the next important source of uncertainty following from the sampling errors we assigned to our data points. The errors in the adopted parameters of Draco concerning the surface distribution of stars, luminosity or distance probably have much smaller effect (see Lokas 2002).

The joint fitting of the velocity dispersion and kurtosis for the sample with 189 stars gives results not very different from those indicated by the minimum of χ^2 (thicker dotted line) in the lowest panel of Fig. 3. The best-fitting parameters (with $\chi^2/N = 7.4/10$) are

$$M_D = M_S = 99; \quad r_b = R_S = 1.9; \quad \alpha = 0.4; \quad (24)$$

The best estimate of the total mass of the Draco dwarf is then $6.6 \cdot 10^7 M_\odot$. We emphasize that the result is not robust and could be very different if different stellar samples were taken. Our choice of velocities has been rather arbitrary and one could probably get reasonable results also with slightly larger or smaller samples. One could for example construct samples by removing the stars with most discrepant velocities one by one and performing a similar fitting procedure as described here. One would then get a series of best fitting masses of decreasing values.

The mass estimate found above is significantly smaller than the ones obtained with the NFW mass distribution and older data (Lokas 2002), which were even of the order of $10^9 M_\odot$ for reasonable concentrations. This was due to the more extended nature of the NFW profile, which was modified here by adding an exponential cut-off. Recently, it has been proposed that, if the dwarf spheroidals of the Local Group indeed possess such high masses, then their low abundance could be understood by referring to the cosmological mass function, which predicts many fewer objects with such high mass (Hayashi et al. 2003). Our present lower mass estimate could be consistent with this solution to the overabundance problem if the dwarfs originally indeed had such high masses but were then tidally stripped in the Milky Way potential. Such a scenario could also explain why dwarfs managed to build up their stellar content in presently shallow potential wells (Krauss, Gnedin & Klypin 2004).

Our estimate of Draco's mass is not directly comparable to that of Klypin et al. (2002) since they used different dark matter models and a smaller stellar sample (constructed from an older data set but in a weakly restrictive way similar to our sample with 207 stars). Their best estimate of the mass inside three core radii was $8 \cdot 10^7 M_\odot$, which is, as would be expected, already more than our total mass value.

The velocity moments obtained with the sets of parameters listed in (24) are shown in Fig. 5 together with the data for 189 stars. The dark matter density profile following from equation (21) with those parameters is plotted in Fig. 6 together with the stellar mass density profile $\rho_*(r) = \rho_*(r)$ with $\rho_*(r)$ given by equation (19). Fig. 6 also shows the cumulative mass-to-light ratio, i.e. the ratio of the total mass distribution to the luminosity distribution in the V-band inside radius r

$$M/L_V = \frac{M(r)}{L_V(r)}; \quad (25)$$

where $M(r)$ is the sum of two contributions from stars and dark matter given by equation (23) with (20) and (22), while

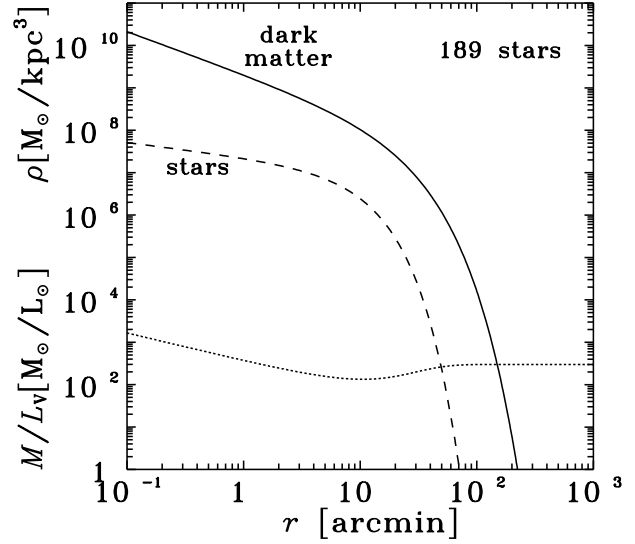


Figure 6. Best fitting dark matter density profile (solid line) in comparison to the stellar mass density profile (dashed line). The dotted line shows the cumulative mass-to-light ratio for the best fitting profile.

$L_V(r) = M(r) = \rho_*(r) + \rho(r)$. The behaviour of this quantity is easily understood: the dark matter cusp is steeper than that of the luminosity distribution therefore the ratio increases towards the centre. This is due to our adopted profile of dark matter halo, which, according to the simulations of Kazantzidis et al. (2004), preserves the NFW cusp. With a steeper dark matter inner slope (as recently proposed by Navarro et al. 2004 and Stoeckl 2005 for global halos, and by Hayashi et al. 2003 for tidally stripped ones), the data may well be reconciled with a constant mass-to-light ratio.

At large distances, the mass-to-light ratio converges to a constant value $\rho_*(1 + M_D/M_S) = 299$ since both luminosity and dark matter distributions fade exponentially. This result is comparable to the estimate by Klypin et al. (2002) who found $M/L_V = 330$ within three core radii, while Odenkirchen et al. (2001), assuming that mass follows light, obtain $M/L_i = 146$. Our result is also consistent with the study of Lokas (2002) using older data, where dark matter was modelled with a generalized NFW distribution. There $M/L_V > 100$ was found at $R > 10$ arcmin, and the mass-to-light ratio was increasing at large radii due to the assumption of an untruncated, $\rho \propto r^{-3}$, dark matter envelope.

Fig. 7 illustrates the uncertainties in the estimated parameters due to the sampling errors of the velocity moments. Here, we plot the cuts through the confidence region in three possible parameter planes with probability contours corresponding to 1 (68 percent confidence), 2 (95 percent) and 3 (99.7 percent) i.e. $\chi^2 = \chi^2_{min} + 2.30, 5.99, 11.83$, where $\chi^2_{min} = 7.4$. Contrary to the case where only the velocity dispersion was fitted, some constraints on parameters can now be obtained, but the allowed ranges of parameters are large. This is especially the case for parameters $M_D = M_S$ and $r_b = R_S$ which are highly degenerate. Since the parameters $M_D = M_S$ and $r_b = R_S$ are very weakly correlated with α , as can be seen from the two upper panels of Fig. 7, the cuts provide a good approximation of the true uncertainties in

the parameters. However, these errors, due to the low number of velocities per bin, are much smaller than uncertainties due to our choice of stars to include in the sample.

As already stated above, we find the preferred stellar orbits to be weakly tangential. For the sample with 189 stars we get the best-fitting $\beta = 0.4$ (corresponding to $\alpha_r = 1.2$) and the expected uncertainties can be read from the two upper panels of Fig. 7. Note that according to the Figure the orbits are consistent with isotropy at 1 level, while a strongly radial or a strongly tangential velocity distribution are ruled out. It must be remembered, however, that these conclusions were reached with the assumption of negligible binary fraction in Draco. As discussed in Section 3, the correction for binaries significantly affects the values of kurtosis (see Fig. 2), but again more so for the sample with 189 stars than for the other samples which have higher values of kurtosis. If the binary fraction in Draco is significant, e.g. of the order of $\beta = 0.5$ as for the solar neighbourhood according to current estimates (Duquennoy & Mayor 1991; De Rijcke & Dejonghe 2002) then the intrinsic kurtosis will be decreased and the inferred orbits even more tangential. Reproducing the velocity dispersion profile (which is not strongly affected by the binaries) would then require a less extended mass distribution and the inferred masses will be even smaller.

We have mentioned before that the main gain from including the kurtosis in the analysis is the ability to constrain the anisotropy of stellar orbits. Interestingly, weakly tangential orbits in Draco appear to be a robust conclusion from our study; whatever the sample of the stars taken and binary fraction assumed the preferred models have $\beta < 0$ or $\alpha_r > 1$. This result seems to contradict the general belief, based e.g. on N-body simulations, that virialized systems should have orbits close to isotropic or even mildly radial (see Mamon & Lokas 2005). However, as discussed by Kazantzidis et al. (2004), tidally stirred stellar populations can develop tangential orbits even when evolving in an isotropic halo.

A possible scenario for the formation of dwarf spheroidal galaxies has been proposed by Mayer et al. (2001) who used high-resolution N-body/SPH simulations to study the evolution of rotationally supported dwarf irregular galaxies moving on bound orbits in the massive dark matter halo of the Milky Way. They showed that the tidal field induces severe mass loss in their halos and the low surface brightness dwarfs are transformed into pressure-supported dwarf spheroidals with preferably tangential orbits outside the centre (see Fig. 25 of the preprint version of Mayer et al. 2001).

Besides, tangential orbits may not be restricted to dwarf spheroidals. A recent study of kinematics of a sample of Virgo Cluster dwarf ellipticals (Geha, Guhathakurta & van der Marel 2002) also shows the preference of tangential orbits and actually the mechanism to produce them may be similar as in the case of dwarf spheroidals (Mayer et al. 2001) only with high surface brightness galaxies as progenitors. Also, elliptical galaxies formed by major mergers of spiral galaxies often show tangential anisotropy in their inner regions (Deke et al. 2005), which is caused by some of the stars having formed within the gaseous disk, which is in nearly circular rotation in the merger remnant.

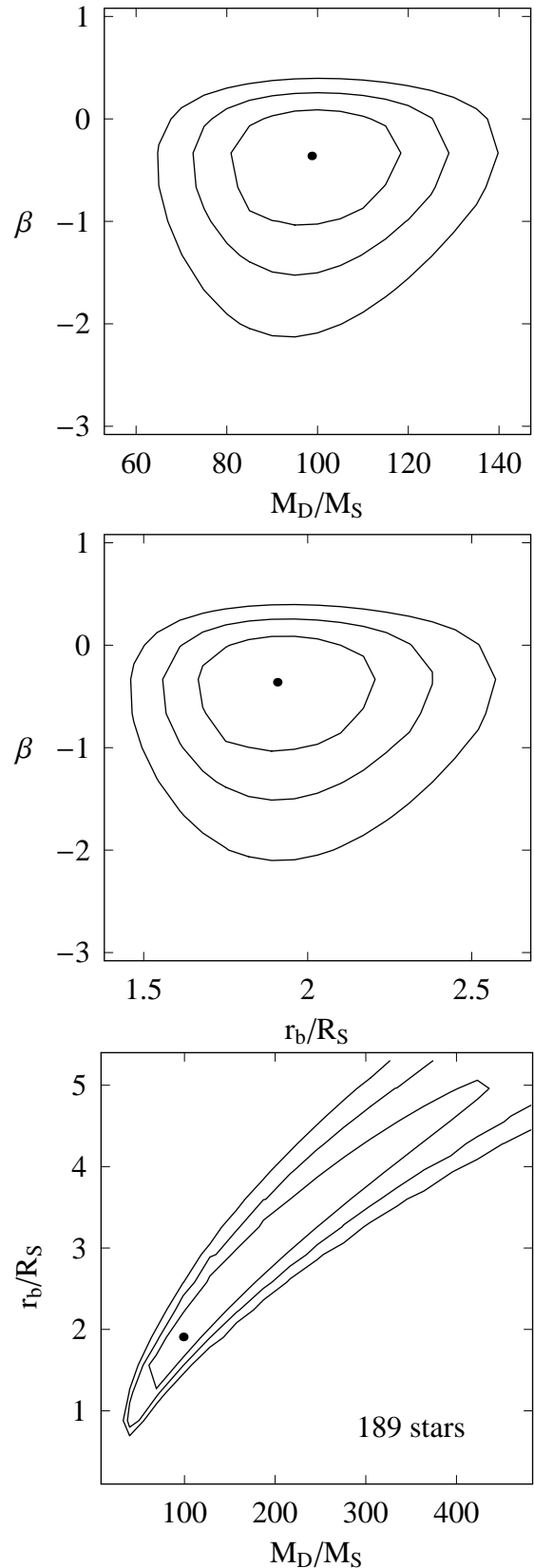


Figure 7. Cuts through the 1, 2 and 3 probability contours in the parameter space obtained from fitting \log_{10} and $(\log_{10})^{1/10}$ for the sample with 189 stars. Dots indicate the best-fitting parameters.

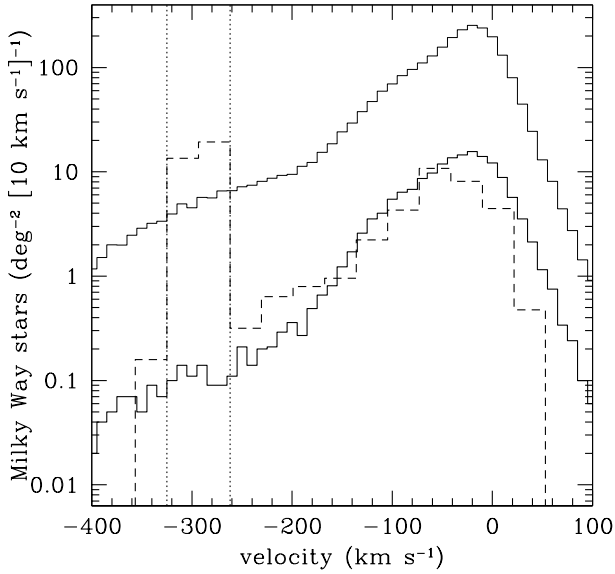


Figure 8. Expected contamination of Draco by Milky Way stars. The diagram shows the expected total number of Milky Way stars of given velocities (higher histogram, thin solid line) and the corresponding number if we restrict ourselves to the red giant branch of the color-magnitude diagram of Draco (lower histogram, thick solid line). The dashed line shows the velocity distribution of stars actually observed in the direction of Draco by Wilkinson et al. (2004). The contamination by giants in the velocity range of Draco, indicated by two vertical dashed lines, is very small.

6 INTERLOPERS FROM THE MILKY WAY OR TIDAL DEBRIS?

We have shown that the main issue in the analysis of the velocity moments is the question of which stars should be included in the analysis, or, to put it in a different way, which of them are unbound and only artificially affect the moments, e.g. in the velocity dispersion. We argued that the presence of unbound stars leads to inconsistent velocity dispersion and kurtosis which cannot both be fitted by equilibrium models following from the Jeans formalism. It is therefore essential to study the possible origin of those unbound stars.

An immediate first guess would be that the stars are the members of the Milky Way. In order to verify this hypothesis we have run the Besancon Galaxy model (Robin et al. 2003, <http://bison.obs-besancon.fr/modele/>) in the direction of Draco, which gives the velocity distribution shown by the higher histogram (thinner solid line) in Fig. 8. If stars of all types are considered, as they are for this histogram, then the expected number of Milky Way interlopers with Draco-like velocities in the range $-325 \text{ km s}^{-1} < v < -262 \text{ km s}^{-1}$, indicated by the two vertical dashed lines in the Figure, would be 15 ± 25 . However, if we restrict the analysis to the red giant branch (RGB) of the Draco color-magnitude diagram with 0.075 mag from the typical trend we end up with a much lower expected number density of stars represented by the lower histogram (thicker solid line) in Fig. 8. Since the observations of Draco stars by Kleya et al. (2002) and Wilkinson et al. (2004) were indeed restricted to RGB stars we expect the contamination from the Milky Way stars to be very small with 1.42 ± 0.17 expected interlopers. The

velocity distribution of all RGB stars observed by Wilkinson et al. (2004) is shown with a dashed line in the plot. We can see that the level of this histogram right outside the range of velocities adopted for Draco stars is somewhat higher than expected from the Besancon model. A naive interpolation of the observed velocity distribution (dashed histogram in Fig. 8) outside of the Draco velocity zone would yield 6.5 ± 2.3 interlopers from the Milky Way.

Given our finding that the kinematic modelling of the 189-star sample yields consistent results, while those of the 207- and 203-star samples do not, the total number of interlopers in Draco is of order of $207 - 189 = 18$ stars. Therefore, given our estimates of the previous paragraph of the number of Milky Way interlopers, an important fraction (probably the majority) of unbound stars in the neighbourhood of Draco dwarf must originate in Draco itself. An obvious mechanism for the production of such stars is the tidal stripping of Draco by the Milky Way potential. Although no clear signature of tidal tails has been identified in the luminosity distribution of Draco (e.g. Klessen et al. 2003), it is still quite possible that the tails are oriented along the line of sight.

Wilkinson et al. (2004) have recently argued that the tidal scenario is only feasible if the mass of Draco is below $5 \times 10^7 M_\odot$ and its dark matter distribution is low outside roughly 30 arcmin. Interestingly, the results of our analysis seem to almost fulfill these requirements: our best estimate of the mass for the sample with 189 stars is $6.6 \times 10^7 M_\odot$ and the dark matter distribution indeed fades at larger distances, as demonstrated by Fig. 6. Wilkinson et al. (2004) also point out that such a tidally detached population of stars should be heated up, which is contradicted by the decreasing velocity dispersion of Draco at large distances, unless only cold stars remain which are then recaptured by the dwarf. We find that the fall of the velocity dispersion at large angular distances from the centre of Draco is not a very strong feature and its visibility depends on the chosen radial binning of stars.

7 CONCLUDING REMARKS

Given the new data on the Draco dwarf spheroidal, especially the velocity measurements by Kleya et al. (2002) and Wilkinson et al. (2004), we have attempted to constrain the dark matter distribution in Draco by modelling not only the dispersion, but also the kurtosis of the line-of-sight velocity distribution. The analysis of both moments allows us to break the degeneracy between the mass distribution and velocity anisotropy usually present in the analyses of velocity dispersion. Still, many uncertainties remain in the analysis. We show that the results can be very different depending on the sample of stars chosen, i.e. which stars are included in the sample and which are treated as interlopers. Besides, due to the limited number of measured velocities, the sampling errors of the moments are large and the parameters cannot be strongly constrained.

There are few possible remedies to improve the present situation: to have more velocity measurements, to further constrain the dark matter profiles on theoretical grounds and to model the influence of interlopers in more detail. All these approaches seem feasible in the near future. On

the observational side, the measurements of a few hundred velocities per dwarf galaxy are planned or already being performed using large telescopes with multi-fiber spectroscopy like Magellan (M. Mateo, private communication). On the theoretical side, progress might be even faster with the rapidly increasing resolution of the N-body simulations. The recent result of Kazantzidis et al. (2004) itself which we have used in the present work relied on increased resolution to show that the cusp of the dark matter profile is not attenuated due to tidal interaction as was claimed earlier (Stoehr et al. 2002; Hayashi et al. 2003). The result however depended to some extent on the parameters of the orbit of the dwarf around the Milky Way, which in the case of Draco are poorly known.

As for the third issue, the treatment of interlopers or unbound stars, in our opinion this is at present the most important problem in the analysis of the dark matter distribution in dwarf spheroidal galaxies. We have shown that the supposed interlopers can alter the profiles of velocity moments and significantly change the estimated parameters of the dark matter distribution.

ACKNOWLEDGEMENTS

We are grateful to M. Wilkinson and collaborators for sharing with us their new velocity measurements for Draco prior to publication. We wish to thank E. Grebel, J. Kaluzny, S. Kazantzidis, J. Kleyna, A. Klypin, J. Mikolajewska, A. Olech, K. Stanek, F. Stoehr, and especially M. Wilkinson for discussions and comments, and an anonymous referee for suggestions which helped to improve the paper. EL is grateful for the hospitality of Institut d'Astrophysique de Paris and Instituto de Astrofísica de Andalucía in Granada where part of this work was done. We made use of the Besancon Galaxy model available at <http://besancon.frm.odele/>. This research was partially supported by the Polish Ministry of Scientific Research and Information Technology under grant 1P03D 02726, the Jumelage program Astronomie France-Pologne of CNRS/PAN and the exchange program of CSIC/PAN.

REFERENCES

Aparicio A., Carrera R., Martínez-Delgado D., 2001, *AJ*, 122, 2524
 Binney J., Tremaine S., 1987, *Galactic Dynamics*. Princeton Univ. Press, Princeton, chap. 4.
 Bonanos A. Z., Stanek K. Z., Szentgyorgyi A. H., Sasselov D. D., Bakos G. A., 2004, *AJ*, 127, 861
 Derijcke S., Dejonghe H., 2002, *MNRAS*, 329, 829
 Dekel A., Stoehr F., Mamon G. A., Cox T. J., Novak G., Primack J. R., 2005, *Nat*, in press, astro-ph/0501622
 Diem and J., Moore B., Stadel J., 2004, *MNRAS*, 352, 535
 Duquenois A., Mayorm M., 1991, *A&A*, 248, 485
 Fukugita M., Shimazaki K., Ichikawa T., 1995, *PASP*, 107, 945
 Gallagher J. S., Madsen G. J., Reynolds R. J., Grebel E. K., Smekker-Hane T. A., 2003, *ApJ*, 588, 326
 Geha M., Guhathakurta P., van der Marel R. P., 2002, *AJ*, 124, 3073
 Gerhard O. E., 1993, *MNRAS*, 265, 213
 Hayashi E., Navarro J. F., Taylor J. E., Stadel J., Quinn T., 2003, *ApJ*, 584, 541
 Irwin M., Hatzidimitriou D., 1995, *MNRAS*, 277, 1354
 Kazantzidis S., Agorrián J., Moore B., 2004, *ApJ*, 601, 37

Kazantzidis S., Mayer L., Mastropietro C., Diem and J., Stadel J., Moore B., 2004, *ApJ*, 608, 663
 Kleessen R. S., Kroupa P., 1998, *ApJ*, 498, 143
 Kleessen R. S., Zhao H., 2002, *ApJ*, 566, 838
 Kleessen R. S., Grebel E. K., Harbeck D., 2003, *ApJ*, 589, 798
 Kleyna J. T., Wilkinson M. I., Evans N. W., Gilmore G., 2002, *MNRAS*, 330, 792
 Klypin A., Klytsov A. V., Valenzuela O., Prada F., 1999, *ApJ*, 522, 82
 Lin and G. B., Gerbal D., Marquez I., 1999, *MNRAS*, 309, 481
 Lokas E. L., 2001, *MNRAS*, 327, 21P
 Lokas E. L., 2002, *MNRAS*, 333, 697
 Lokas E. L., Mamon G. A., 2003, *MNRAS*, 343, 401
 Mamon G. A., Lokas E. L., 2005, *MNRAS*, in press, astro-ph/0405491
 Mateo M., 1997, in Amaldi M. et al., eds, *ASP Conf. Ser. Vol. 116, The Nature of Elliptical Galaxies*. Astron. Soc. Pac., San Francisco, p. 259
 Mayer L., Goumamoto F., Colpi M., Moore B., Quinn T., Wadsley J., Stadel J., Lake G., 2001, *ApJ*, 559, 754, a slightly different version at astro-ph/0103430
 Merrifield M. R., Kent S. M., 1990, *AJ*, 99, 1548
 Navarro J. F., Frenk C. S., White S. D. M., 1997, *ApJ*, 490, 493 (NFW)
 Navarro J. F. et al., 2004, *MNRAS*, 349, 1039
 Odenkirchen M. et al., 2001, *AJ*, 122, 2538
 Piatek S., Pryor C., Amendro T. E., Olszewski E. W., 2002, *AJ*, 123, 2511
 Prada F. et al., 2003, *ApJ*, 598, 260
 Robin A. C., Reyle C., Derrière S., Picaud S., 2003, *A&A*, 409, 523
 Sanchis T., Lokas E. L., Mamon G. A., 2004, *MNRAS*, 347, 1198
 Schulz J., Fritze-v. Alvensleben U., Møller C. S., Fricke K. J., 2002, *A&A*, 392, 1
 Sersic J. L., 1968, *Atlas de Galaxies Australes*, Observatorio Astronómico, Córdoba
 Stoehr F., 2005, *MNRAS*, submitted, astro-ph/0403077
 Stoehr F., White S. D. M., Tormen G., Springel V., 2002, *MNRAS*, 335, 84P
 van der Marel R. P., Agorrián J., Carlberg R. G., Yee H. K. C., Ellingson E., 2000, *AJ*, 119, 2038
 Wilkinson M. I., Kleyna J. T., Evans N. W., Gilmore G. F., Irwin M. J., Grebel E. K., 2004, *ApJ*, 611, L21
 Wojtak R., Lokas E. L., Göttober S., Mamon G. A., 2005, *MNRAS*, 361, L1